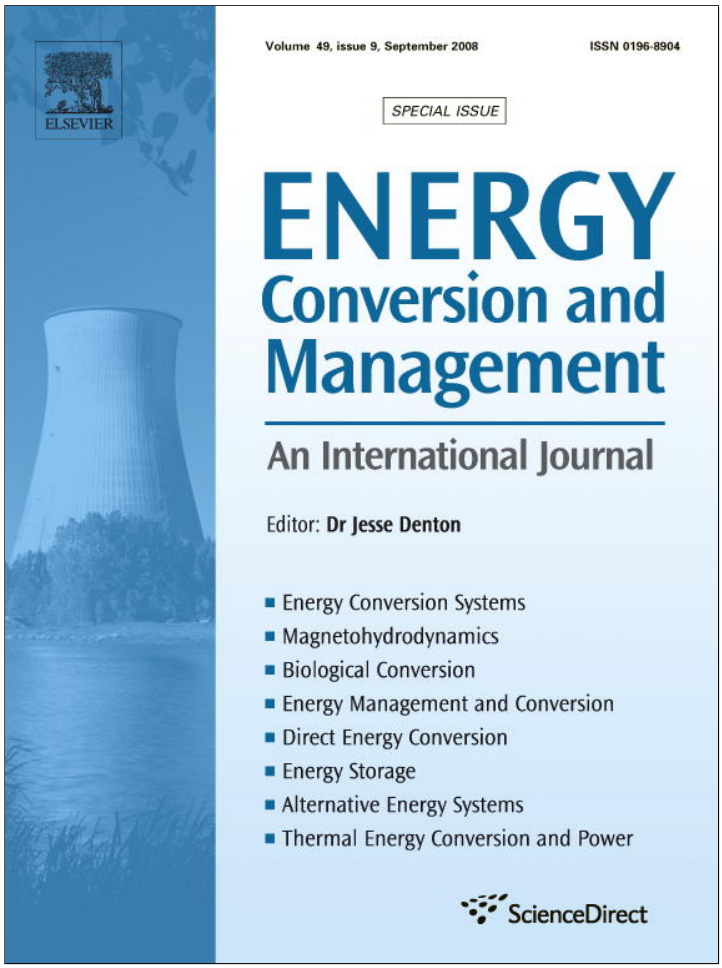

Energy Conversion and Management 49 (2008) 2494–2498

Contents lists available at ScienceDirect

Energy Conversion and Management

journal homepage: www.elsevier.com/locate/enconman

β irradiation effects in graphite and applications to material engineering

P. Szroeder [a,*], A. Chruścińska [a], K. Przegiętka [a], S. Kulesza [b]

[a] Nicolaus Copernicus University, Institute of Physics, Grudzia˛dzka 5/7, 87-100 Toruń, Poland
[b] University of Warmia and Mazury, Faculty of Mathematics and Computer Sciences, Żołnierska 14, 10-561 Olsztyn, Poland

ARTICLE INFO

Article history:
Received 19 October 2007
Accepted 4 January 2008
Available online 15 May 2008

Keywords:
Highly oriented pyrolitic graphite
Surface defects
Sorption capability
Thermally stimulated light emission
Surface resistivity

ABSTRACT

An investigation has been made of graphite exposed to moderate doses (90 Gy–92 kGy) of β irradiation from the point of view of applications to material engineering. The average energy of the β particles was 196 keV. In STM images no significant modification of surface topography was observed. Irradiated samples reveal weak thermally stimulated emission (TSE) signal. Irradiation effects are also hard detectable in EPR and IR spectra. On the other hand, even small radiation doses influence high temperature surface resistance characteristics in ambient air. This result suggests an alteration of surface properties under low irradiation doses.

1. Introduction

Irradiation-induced defects can be used in a beneficial way for altering the properties of carbon materials. The surface modifications should enhance the compatibility of the graphite derived materials for dispersion in polymers and create well-bonded interfaces with the polymer matrix. Nowadays, biosensors are prepared from a composite consisting of graphite and biomaterials [1]. The application of irradiation could have beneficial effects on the target properties of these devices. Irradiation-modified graphitic carbon can be used as anode material for lithium ion batteries [2–4]. There is also a real possibility of developing the irradiation-modified carbon nanomaterials for the hydrogen storage. The chemical and physical sorption processes in nanographite are rate-limited by the hydrogen diffusion transport micromechanisms [5]. Both physical and chemical sorption can be enhanced by introducing stable defects into carbon material. The changes of magnetic properties in modified graphene layers have recently been also confirmed [6–8].

The tendency of graphite to change its structure under irradiation can be exploited in both material and biological settings. However, the stability of irradiation-induced defects is a key to fabrication new materials based on modified graphite. The phenomena of defect formation and recombination in carbon honeycomb structures are the subject of numerous theoretical works [9–15]. Carbon atoms knocked from the graphite lattice produce interstitial (*I*) and vacancy (*V*) defects which tend to form more complex structures. Most of these structures spontaneously relax into metastable intimate *I*–*V* complex (Frenkel pair), perfect graphite or Stone–Wales defect (associated with the rotation of C–C bond within graphene plane). The transformation of defects into the lower energy configurations are presented in a diagram in Fig. 1.

Due to lower migration energy to overcome (0.47 eV) interstitials are more active in relaxation processes. The migration energy of vacancy is 1.7 eV [15]. To recombine, the intimate pair have to overcome the 1.4 eV barrier [14]. This theoretical value corresponds with the experimental value of an activation energy of the Wigner energy release observed in calorimetric experiments at 200 °C [16,17]. The processes of defect relaxation were also examined by temperature Raman measurements giving somewhat lower activation energy of 0.9 eV [18]. Similar value of activation energy was obtained on the base of thermally stimulated light emission experiments [19].

Most of the hitherto published experimental works about electron irradiation effects in graphite concern the question of the electron beam influence on specimen in high resolution transmission electron microscopes. In this study we focus on the effects of 90 Gy–92 kGy doses of β irradiation. Controllable modification of the graphite can extend the field of application of a wide class of carbon materials in chemical engineering. This work has also in view to verify the results of the former TSE study of graphite exposed to β irradiation [19].

2. Experimental

Both the highly oriented pyrolytic graphite (HOPG Grade ZYB, GE Advanced Ceramics) and the graphite powder (Matthey Graphite Powder, 99.9% pure, mean diameter less than 10 μm) were

* Corresponding author. Tel.: +48 566113250; fax: +48 566225397.
E-mail address: psz@fizyka.umk.pl (P. Szroeder).

0196-8904/$ - see front matter © 2008 Elsevier Ltd. All rights reserved.
doi:10.1016/j.enconman.2008.01.038

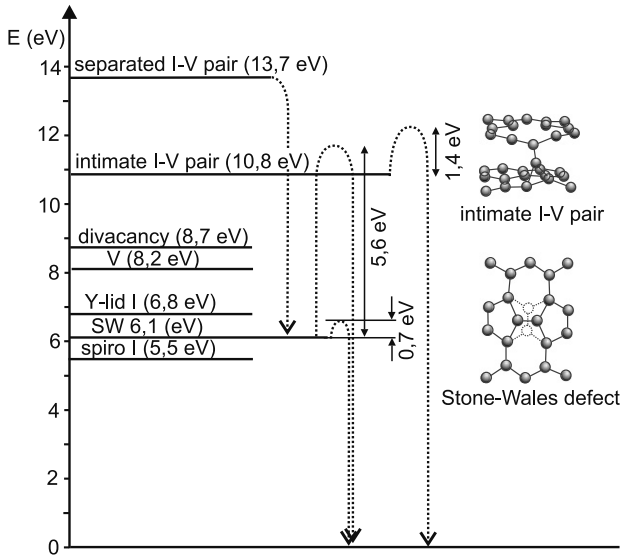

Fig. 1. Diagram of the formation energy of selected defects with respect to ideal graphite crystal lattice. Threefold coordinated interstitial atom is marked with 'Y-lid I', fourfold with 'spiro I'. Activation energies of relaxation processes are also marked. Relaxation of Stone–Wales defects (SW) requires to overcome the 5.6 eV energy barrier. Additional interstitial atom lowers the energy barrier to 0.7 eV. Prepared on the base of calculations presented in [13,14].

irradiated using $^{90}Sr/^{90}Y$ radioactive source. The activity of ^{90}Sr was 1.16 GBq. The calibration of the dose rate was carried out on quartz grain samples producing a result of 50 mGy s^{-1}. This value could also be used as a rough estimate for graphite samples. The average energy of β particles emitted by ^{90}Sr source is 196 keV, giving the penetration depth in graphite of $\sim$300 μm.

STM measurements were made at room temperature using an Omicron microscope (base pressure 7×10^{-8} Pa) with the platinum probe working in a constant tunnelling current mode. Tunnelling current from 0.5 to 2.0 nA with a sample bias from −1.5 to +0.5 V with respect to the tip was used.

The thermally stimulated light emission measurements were carried out using the commercial RisøOSL-TL-DA 12 System. Heating was realized in pure argon flow immediately after the irradiation. Aliquots of 5 mg samples were prepared on thin nickel discs.

DC electrical characteristics were measured in a flat configuration with a two-point platinum contact probe using Keithley 6517 electrometer. Temperature-dependent resistance characteristics in vacuum of 0.13 Pa were probed at voltage of 0.1 V (ohmic contact regime). The heating rate was 2 °C/min up to 600 °C.

EPR spectra were recorded using a Bruker B-ER-418S spectrometer with rectangular resonance cavity (TE_{102} mode) operating in X band (9.3 GHz) with modulation of 100 kHz.

Infrared spectra were obtained on Specord M-80 apparatus with a resolution of 2 cm^{-1}. Samples of graphite powder were run as pressed KBr pellets.

3. Results and discussion

Fig. 2 shows STM images of pristine and β-irradiated HOPG surface. The STM images reflect the charge density at the Fermi level. The corresponding states (darkened area) are p_z states centred at the β sites. It is noticed that from the topographical point of view both the pristine and modified samples appear regular. However, in modified graphene planes the local irregularities caused by the rehybridization of carbon orbitals in graphite crystal are seen.

The result of the TSE experiments are glow curves obtained during irradiation-heating cycles which are presented in Fig. 3.

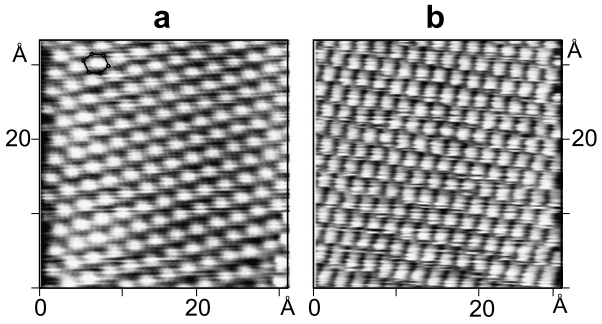

Fig. 2. STM images of pristine HOPG (a) and HOPG after 18 cycles of β irradiation (dose of 90 Gy) and heating up to 500 °C (b).

Heating without prior irradiation produced only incandescence, which revealed transient character of the TSE and indispensable role of irradiation in this phenomenon. A conventional glow curve shape analysis was carried out. If we assume that the observed emission was produced by the first order kinetics process the glow curve can be treated as a sum of components described by following formula [19]:

$$I(T) = n_0 s \exp\left(\frac{-E}{kT}\right) \exp\left(-\frac{s}{\beta}\int_{T_0}^{T} \exp\left(-\frac{E}{kT}\right) dT'\right), \quad (1)$$

where I is the emission intensity, n_0 denotes the initial concentration of defects which participate in TSE process, E is the activation

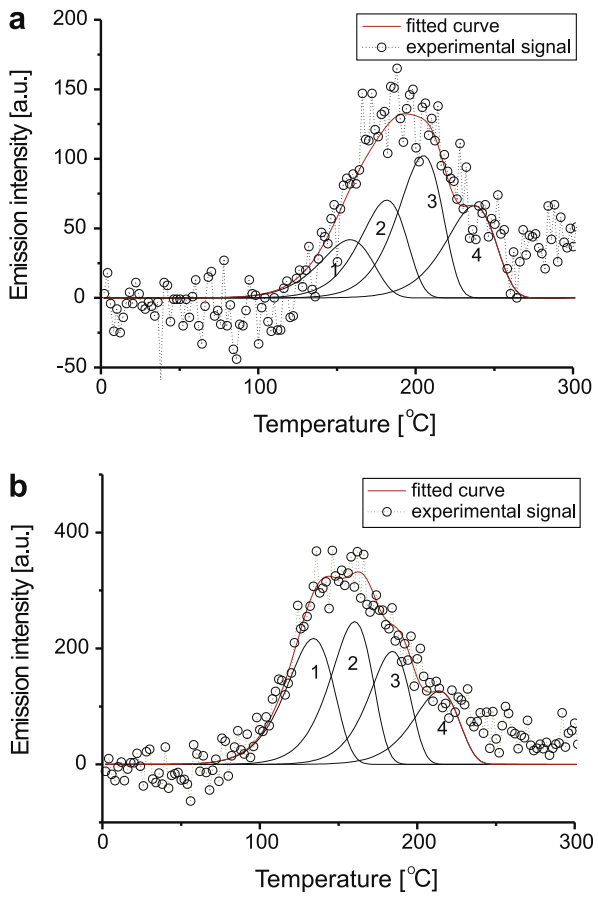

Fig. 3. (a) Glow curve of HOPG subjected to 11 kGy dose of the β radiation measured with a heating rate of 10 °C s^{-1}. (b) Glow curve obtained after delivering 9-2 kGy of the β radiation to the sample in argon ambient gas recorded with a heating rate of 2 °C s^{-1}. In both plots the background signal is subtracted.

energy, s is the pre-exponential (frequency) factor, T the absolute temperature, k the Boltzmann's constant, and β the heating rate.

Fitting the sum of functions (1) to the experimental TSE curves obtained with different heating rates yields exactly the same set of values (E_i, s_i): $E_1 = 0.93$ eV and $s_1 = 4.1 \times 10^{10}$ s^{-1}, $E_2 = 1.20$ eV and $s_2 = 1.2 \times 10^{13}$ s^{-1}, $E_3 = 1.38$ eV and $s_3 = 2.5 \times 10^{14}$ s^{-1}, $E_4 = 1.40$ eV and $s_4 = 4.2 \times 10^{13}$ s^{-1}. Compared to the previous experiments [19], the doses used for producing the TSE signal were significantly higher. The difference in the sensitivity to radiation dose can be explained by the various quality of material delivered by different companies. That is why this technique should be cautiously applied to the sp^2-bonded carbon materials.

The temperature-dependent surface resistance of the HOPG measured in ambient air and vacuum is drawn in Fig. 4a and b. The resistance of the pristine HOPG falls down with the increasing temperature. The semiconductor-like behaviour in the studied range of temperatures allows us to apply simple model for determining an activation energy of the conduction electrons. The temperature dependence of resistance in semiconductors is given by

$$\ln\frac{R}{R_0} \simeq \frac{E_a}{kT}, \tag{2}$$

where R is the resistance, R_0 the parameter depending on the material, E_a the activation energy, k the Boltzmann's constant and T the absolute temperature. Thus, E_a can be estimated from a slope of the resistance curve drawn in the Arrhenius plot. The resistance changes in the case of graphite respond to a very low activation energy of 20 meV. However, after exposition of the sample to the 90 Gy dose of β radiation the significant change of temperature characteristic is observed. Within the low temperature range ($T < 120$ °C) the resistance increases with the temperature giving metallic dependence. When the same sample is subjected to the next dose of irradiation after the heating cycle, the change of resistance character is observed in 80 °C. The same effect is observed after subsequent exposition to β radiation. Repeated heating leads to further lowering of the transition temperature to 60 °C. Another characteristic of the temperature resistance dependence recorded in ambient air is the change of the Arrhenius plot slope at 190 °C that corresponds with a jumping of the activation energy from 26 to 100 meV.

On the other hand, the temperature dependence of the surface resistance in vacuum does not change even if the irradiation dose exceeds 40 times the doses applied before measurements carried out in ambient air. In this case, the activation energy of the conduction electrons does not change being 19 meV. The results prove

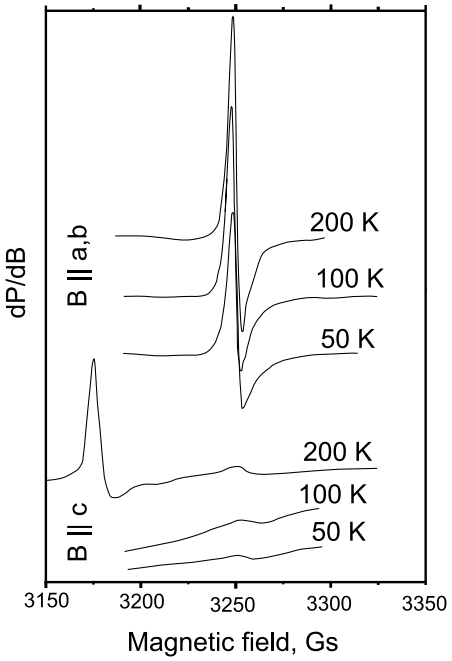

Fig. 5. EPR spectra of HOPG after 18 cycles of β irradiation (dose of 90 Gy) and heating (up to 500 °C) with static magnetic field perpendicular and parallel to the crystallite c-axis.

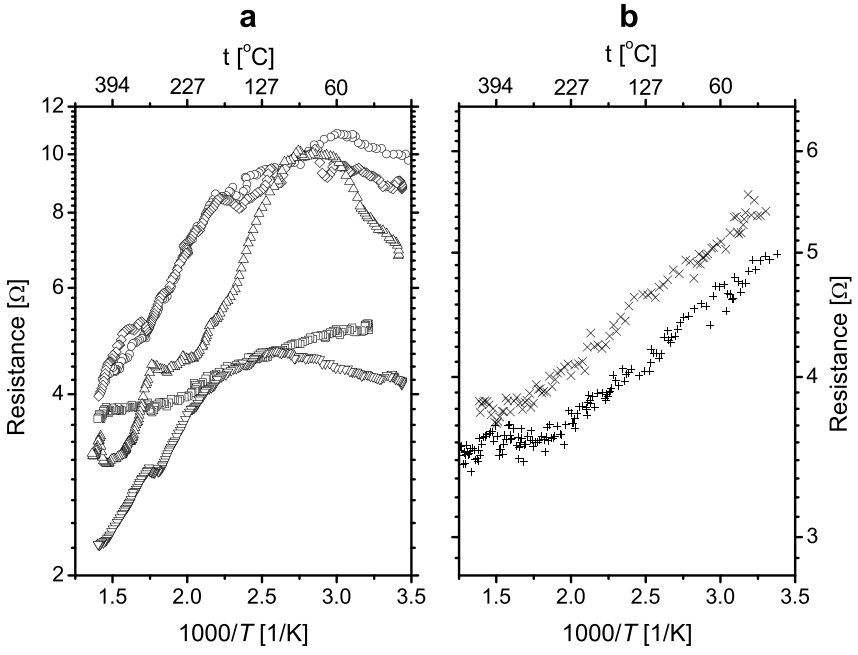

Fig. 4. Arrhenius plot of the temperature-dependent surface electrical resistance of the β-irradiated HOPG measured in ambient air (a) and in vacuum of 10^{-1} Pa (b). Squares, pristine HOPG; upside-down triangles, HOPG after delivering the first dose of irradiation; triangles, the second dose delivered to the same sample; diamonds, third dose; circles, next heating cycle after third dose (each dose is of 90 Gy); +, pristine HOPG; ×, HOPG exposed to the 3.5 kGy dose of β irradiation.

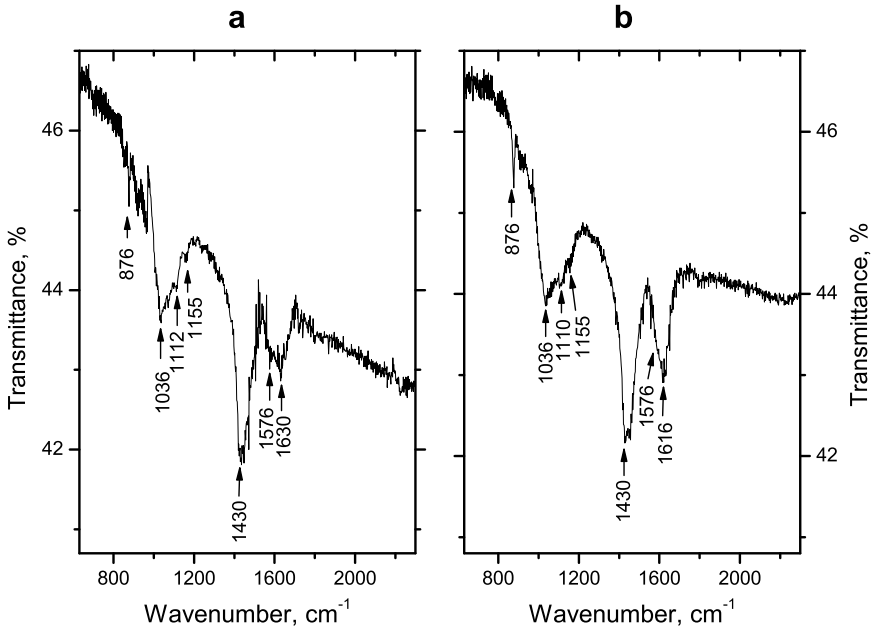

Fig. 6. Infrared spectra of the pristine graphite powder (a) and the sample exposed to 13 kGy of β irradiation (b).

that surface defects induced by β irradiation are chemically stabilized by atmospheric air. Hence, we can conclude that β irradiation enhances sorption capability of graphite. The changes of the resistance slope indicate the relaxation processes of defects to take place at definite temperatures. In particular, the deflection observed at 190 °C coincides with one of the peaks observed in glow curves.

The EPR spectra (Fig. 5) of graphite exposed to β irradiation reveal an anisotropy of the g factor. At room temperature their value varies from 2.0026 to 2.05 as the magnetic field direction changes from perpendicular to parallel to the c-axis. The g factor in the magnetic field parallel to the c-axis increases with decreasing temperature and reaches the value 2.14 at 50 K (the resonance line not seen within the range of magnetic fields displayed in Fig. 5). These experimental facts rather reproduce the EPR behaviour of pristine HOPG [20]. The only effect of the β irradiation is a very weak line observed in the parallel orientation ($g = 2.0024$) which can be attributed to localized magnetic moments.

Fig. 6 displays the IR spectra of the pristine and the β-irradiated graphite powder. Exposition of the sample to the comparatively strong radiation dose of 13 kGy does not introduce any significant changes in the absorption spectrum. Two weak peaks characteristic of graphite at 876 (A_{2u} mode) and 1576 cm^{-1} (E_{1u} mode) are present. The peaks in the region 1036–1155 cm^{-1} are indicative of C=C=O and C–OH stretching of functional groups attached to the surface of graphite grains. The peak at 1430 cm^{-1} corresponds to the C=O stretching of the carboxyl group [21]. The spectra also show a C=C peak at 1630 cm^{-1} which is downshifted in irradiated sample to the position at 1616 cm^{-1}. Note that intensity of this peak slightly increases after irradiation indicating presence of an electronegative substituent.

4. Conclusions

The results of STM, TSE, surface resistance, EPR and IR measurements of HOPG and graphite powder exposed to β irradiation were presented. The TSE signal was detected but its intensity was lower than intensities observed in previous experiments [19]. No significant changes in the electron paramagnetic resonance spectra were seen in the irradiated samples. This proves that the applied irradiation doses do not modify electronic structure of graphite near Fermi level and localized spin states connected with the β induced defects are rather sparse.

From the point of view of material engineering, fast identification of surface defects in sp^2-bonded carbon materials is the critical point for controllable surface modification. However, the TSE technique tested in this study gives incomplete insight into processes of defects formation and transformation. Moreover, this technique cannot be efficiently applied to examination of unstable defects which are formed during β irradiation.

Graphite in which TSE is observed is characterized by a small band gap (between 10 and 20 meV). Therefore surface defects induced by β irradiation as well as their transformations play an essential role in the light emission mechanism. The results of electrical surface resistance measurements indicate several directions for further experiments.

References

[1] Gilmartin MA, Hart JP. Sensing with chemically and biologically modified carbon electrodes. A review. Analyst 1995;120(4):1029–45.
[2] Wu YP, Holze R. Anode materials for lithium ion batteries obtained by mild and informly controlled oxidation of natural graphite. J Solid State Electrochem 2003;8(1):73–8.
[3] Buqua H, Goers D, Spahr ME, Novak P. The influence of graphite surface modification on the exfoliation during electrochemical lithium insertion. J Solid State Electrochem 2003;8(1):79–80.
[4] Endo K, Zhang HP, Fu LJ, Lee KJ, Sekine K, Takamura T, et al. Electrochemical performance of a novel surface modified spherical graphite as anode material for lithium ion batteries. J Appl Electrochem 2006;36(11):1307–10.
[5] Waqar Z, Denisov EA, Kompaniets TN, Makarenko IV, Titkov AN. Modification of graphite surface in the course of atomic hydrogen sorption STM and AFM study. Phys Scr 2001;T94:132–4.
[6] Höhne R, Esquinazi P. Can carbon be ferromagnetic. Adv Mater 2002;14(10):753–6.
[7] Han K, Spemann D, Esquinazi P, Höhne R, Riede V, Butz T. Ferromagnetic spots in graphite produced by proton irradiation. Adv Mater 2003;15(20):1719–22.
[8] Lehtinen PO, Foster AS, Ayuela A, Krasheninnikov A, Nordlund K, Nieminen RM. Magnetic properties and diffusion of adatoms on graphene sheet. Phys Rev Lett 2003;91(1):017202.
[9] Zunger A, Englman R. Self-consistent LCAO calculation of the electronic properties of graphite. II. Point vacancy in the two-dimensional crystal. Phys Rev B 1978;17(2):642–61.
[10] Banhart F. Irradiation effects in carbon nanostructures. Rep Prog Phys 1999;62(8):1181–221.

[11] Nicholson APP, Bacon DJ. Distortion of the graphite lattice by a vacancy: a two-dimensional model. Phys Stat Solidi A 1975;28(28):613–25.
[12] Hjort M, Stafström S. Modelling vacancies in graphite via the Hückel method. Phys Rev B 2000;61(20):14089–94.
[13] Telling RH, Ewels CP, El-Barbary AA, Heggie MI. Wigner defects bridge the graphite gap. Nature Mater 2003;2(5):333–7.
[14] Ewels CP, Telling RH, El-Barbary AA, Heggie MI. Metastable Frenkel pair defect in graphite: source of Wigner energy? Phys Rev Lett 2003;91(2):025505.
[15] El-Barbary AA, Telling RH, Ewels CP, Heggie MI, Briddon PR. Structure and energetics of the vacancy in graphite. Phys Rev B 2003;68(13):144107.
[16] Mitchell EWJ, Taylor MR. Mechanism of stored-energy release at 200 °C in electron irradiated graphite. Nature 1965;208(13):638–41.
[17] Iwata T. Fine structure of Wigner energy release spectrum in neutron irradiated graphite. J Nuclear Mater 1985;133–134:361–4.
[18] Asari E, Kitajima M, Nakamura KG. Thermal relaxation of ion-irradiation damage in graphite. Phys Rev B 1993;47(17):11143–8.
[19] Chruścińska A, Przegiętka KR, Szroeder P, Oczkowski HL, Rozpłoch F. Luminescence from β irradiated graphene layers. Acta Phys Pol A 2006;110(1):71–80.
[20] Matsubara K, Tsuzuku T, Sugihara K. Electron spin resonance in graphite. Phys Rev B 1991;44(21):11845–51.
[21] Tobin MC. Laser Raman spectroscopy. New York, London, Sydney, Toronto: Wiley-Interscience; 1971. p. 9–104.